ANTIOXIDANTS & REDOX SIGNALING
Volume 15, Number 6, 2011

DOI: 10.1089/ars.2010.3553

Absence of Tumor Suppressor Tumor Protein 53-Induced Nuclear Protein 1 (TP53INP1) Sensitizes Mouse Thymocytes and Embryonic Fibroblasts to Redox-Driven Apoptosis

Prudence N'guessan,[1,2] Laurent Pouyet,[1,2] Gaëlle Gosset,[1–3] Sonia Hamlaoui,[1,2] Marion Seillier,[1,2] Carla E. Cano,[1,2] Mylène Seux,[1,2] Pierre Stocker,[3] Marcel Culcasi,[3] Juan L. Iovanna,[1,2] Nelson J. Dusetti,[1,2] Sylvia Pietri,[3] and Alice Carrier[1,2]

Abstract

The p53-transcriptional target TP53INP1 is a potent stress-response protein promoting p53 activity. We previously showed that ectopic overexpression of TP53INP1 facilitates cell cycle arrest as well as cell death. Here we report a study investigating cell death in mice deficient for TP53INP1. Surprisingly, we found enhanced stress-induced apoptosis in TP53INP1-deficient cells. This observation is underpinned in different cell types *in vivo* (thymocytes) and *in vitro* (thymocytes and MEFs), following different types of injury inducing either p53-dependent or -independent cell death. Nevertheless, absence of TP53INP1 is unable to overcome impaired cell death of p53-deficient thymocytes. Stress-induced ROS production is enhanced in the absence of TP53INP1, and antioxidant NAC complementation abolishes increased sensitivity to apoptosis of TP53INP1-deficient cells. Furthermore, antioxidant defenses are defective in TP53INP1-deficient mice in correlation with ROS dysregulation. Finally, we show that autophagy is reduced in TP53INP1-deficient cells both at the basal level and upon stress. Altogether, these data show that impaired ROS regulation in TP53INP1-deficient cells is responsible for their sensitivity to induced apoptosis. In addition, they suggest that this sensitivity could rely on a defect of autophagy. Therefore, these data emphasize the role of TP53INP1 in protection against cell injury. *Antioxid. Redox Signal.* 15, 1639–1653.

Introduction

In eukaryotic organisms, cells are continually exposed to intrinsic and extrinsic damage that can alter their integrity and drive them to become cancerous cells. They evade from this outcome thanks to a well-adapted stress response which involves molecular events, in particular, induced expression or activation of stress proteins, followed by cellular events, mainly cell cycle arrest allowing damage repair and apoptosis if the stress persists or is too intense to resolve. Accordingly, cell cycle arrest/senescence and apoptosis are the main mechanisms of tumor suppression. One of the best-known and most important tumor suppressor is p53, whose protective activity is missing in more than 50% of human tumors owing to gene mutations. Upon stress, expression and activity of p53 are induced, leading to a cascade of gene expression and protein activity modulations contributing to stress damage avoidance.

During the last decade, we demonstrated the importance of Tumor Protein 53-Induced Nuclear Protein 1 (TP53INP1) as a key stress-response protein. The gene encoding TP53INP1 is a transcriptional target of p53 (31, 43) and of other transcription factors such as p73 and E2F1 (18, 45). Reciprocally, TP53INP1 modulates p53 activity through direct interaction with p53 protein, as well as interaction with the protein kinases HIPK2 and PKCδ which modulate p53 pro-apoptotic activity by phosphorylation (42, 47). We reported that ectopic overexpression of TP53INP1 induces cell cycle arrest and cell death, pinpointing its implication in tumor suppression (44). In addition, we showed that TP53INP1 is lost in human pancreatic and gastric cancer (15, 21), and that its restoration inhibits tumor development owing to cell death induction (15, 21). Importantly,

[1]INSERM, U624 « Stress cellulaire », Marseille, France.
[2]Aix-Marseille Université, Campus de Luminy, Marseille, France.
[3]Sondes Moléculaires en Biologie, Laboratoire Chimie Provence UMR 6264 CNRS-Universités Aix-Marseille I, II & III, Faculté des Sciences de Saint-Jérôme, Marseille, France.

we provided compelling evidence for a function of TP53INP1 in tumor suppression *in vivo* by generating a mouse model for TP53INP1-deficiency in which tumor development is facilitated in three different models of induced tumorigenesis (7, 15, 16).

Downregulation of p53 is associated with an increase in intracellular formation of reactive oxygen species (ROS) and with excessive oxidation of DNA and linked genomic instability (37). Dietary supplementation with the antioxidant *N*-acetylcysteine (NAC) prevents lymphoma development, which is characteristic of p53-deficient mice. Until now, none of the known p53-target genes were able to fully recapitulate the p53-mediated antioxidant response in the p53-deficient cells. Recently, we defined p53-target gene TP53INP1 as a major actor in p53-driven oxidative stress response (7, 16). Indeed, TP53INP1 inactivation induces a persistent accumulation of ROS, as observed for p53 inactivation. Moreover, ectopic expression of TP53INP1 in p53-deficient cells restores a normal redox status. Furthermore, in the absence of TP53INP1, oxidative stress-related lymphoma incidence is markedly increased in $p53^{+/-}$ mice, and oxidative stress-associated carcinogenesis in the colon is promoted. Altogether, these data show that constitutive oxidative stress in the absence of TP53INP1 plays a primary role in facilitating tumorigenesis.

TP53INP1 absence could also promote carcinogenesis by facilitating proliferation. Indeed, proliferation of TP53INP1-deficient fibroblasts is increased (7), which is consistent with the observation that, conversely, ectopic overexpression of TP53INP1 induces cell cycle arrest. Altogether these observations comfort the implication of TP53INP1 as a cell cycle regulator, participating in its tumor suppression function. During the course of this previous study (7), we also demonstrated, by the use of antioxidant complementation, that increased proliferation in TP53INP1-lacking cells relies on their increased level of ROS.

In this study, we address the link between TP53INP1 absence and apoptosis. We previously reported that ectopic overexpression of TP53INP1 induces cell death, suggesting a pro-apoptotic role for TP53INP1. Therefore, TP53INP1 absence could promote carcinogenesis by impairing apoptosis, as is the case for p53. Here we report results showing that, paradoxically, absence of TP53INP1 facilitates cell death, both *in vivo* and *in vitro*, and in two different cell types. Furthermore we demonstrate that constitutive oxidative stress, which is a feature of TP53INP1-deficient cells, is responsible for their sensitivity to induced apoptosis.

Materials and Methods

Mice

We described previously the generation of TP53INP1-deficient mice on a mixed C57BL/6×129/Sv genetic background and their genotyping by PCR with primers (16). Mice were then backcrossed on the C57BL/6 parental genetic background for nine generations. All mice used during the course of this study, including p53-deficient mice (kindly provided by Tak Mak, Campbell Family Institute for Breast Cancer Research, Toronto, Canada) were on C57BL/6 genetic background. Mice, both males and females, were analyzed between 6 and 8 weeks of age. All mice were kept within the animal facilities and according to the policies of the Laboratoire d'Exploration Fonctionnelle de Luminy (Marseille, France). To induce *in vivo* thymocyte death, age- and sex-matched mice were whole-body irradiated at 6 Gy (600 rad) in the Immunology Center of Marseille-Luminy irradiation device (1.28 Gy/min–Year 2009), or intraperitoneally injected with dexamethasone (200 μg) dissolved in PBS (Sigma-Aldrich, France).

Cells

Thymocytes were obtained from whole thymus by teasing across a sterile nylon membrane and cultured in DMEM, 10% (v/v) fetal bovine serum (FBS; Invitrogen, Carlsbad, CA) at 37°C, 5% CO_2. For cell death experiments, thymocytes were plated in triplicate in 96-well plates (1 million cells by well), and either left untreated (spontaneous death) or irradiated (0.5 Gy) or treated with dexamethasone (1 n*M*).

Preparation of transformed mouse embryonic fibroblasts (MEFs) was previously reported (15). In the current study, we used embryos on the C57BL/6 genetic background. MEFs were plated in triplicate in 12-well plates (100,000 cells per well), irradiated (10 Gy) 2 days later, and apoptosis was assessed 24 h later.

When specified, culture medium was complemented with 20 mmol/l NAC (Sigma-Aldrich).

QRT-PCR

Expression of the gene encoding TP53INP1 was quantified by real-time RT-PCR. RNA was obtained from thymocytes 6 h after whole-body irradiation (6 Gy) or intraperitoneal injection of dexamethasone (200 μg) by the TRIzol technique (Invitrogen). cDNAs were prepared using Improm-II kit following the manufacturer's instructions (Promega Corp. Madison, WI). Quantitative PCR was performed in a MX3005P machine (Stratagene, Santa Clara, CA) using the SYBR Premix Ex Taq and ROX reference dye (Takara Bio, Otsu, Shiga, Japan). Amplification consisted in an initial denaturation 10 sec at 95°C, followed by cycles of 8 sec denaturation at 95°C, 15 sec annealing at 55°C, and 30 sec of extension at 72°C. TP53INP1 expression was normalized by the expression of TBP (TATA box Binding Protein) and by the delta CT method ($2^{-(\Delta\Delta Ct)}$). $\Delta\Delta Ct = (Ct\ target\ gene - Ct\ normalizer)_{sample\ control\ (calibrator)} - (Ct\ target\ gene - Ct\ normalizer)_{sample\ treated}$. The primer sequences for each gene are TP53INP1-F: 5′-GTG TGC TCT GCT GAG GAC TC-3′ and TP53INP1-R: 5′-GTT GAC TTC ATA GAT ACC TGC CC-3′; TBP-F: 5′-GGG AGA ATC ATG GAC CAG AA-3′ and TBP-R: 5′-CCG TAA GGC ATC ATT GGA CT-3′. See Supplementary Data (Supplementary Data are available online at www.liebertonline.com/ars).

Flow cytometry experiments

Thymocytes analysis. Thymocytes were prepared from thymus and stained at 4°C in FACS Buffer (PBS, FBS 3%, sodium azide 0.02%) with fluorescent-labeled anti-CD4 and anti-CD8 antibodies (BioLegend, San Diego, CA). Stained cells were analyzed on a FACSCalibur flow cytometer (BD Biosciences, San Jose, CA). Data analysis was performed using CellQuest (BD Biosciences) or FlowJO (Treestar, Ashland, OR) software.

Apoptosis assays. All analyses of apoptotic cell death were done at a single cell level by flow cytometry on the

FACSCalibur flow cytometer. To study mitochondrial membrane permeabilization, cells were incubated with 100 nmol/l 3,3′-dihexyloxacarbocyanine iodide ($DiOC_6$, Molecular Probes, Eugene, OR) for 30 min. Apoptotic DNA fragmentation was determined by measuring the DNA content of individual cells with propidium iodide staining. At the indicated time point, cells were washed once with PBS and fixed in 70% ethanol/PBS for 30 min at 4°C. Cells were then washed twice in PBS and incubated with 100 μg/ml DNase-free RNase (Sigma-Aldrich). Thereafter cells were resuspended in PBS containing 50 μg/ml propidium iodide (Sigma-Aldrich) and analyzed by flow cytometry. For measurement of caspase activation, a FITC-labeled conjugate of the cell-permeable pan caspase inhibitor valyl-alanyl-aspartyl-(*O*-methyl)-fluoromethylketone (VADfmk; Promega) was incubated with cells in PBS during 30 min at 37°C, 5% CO_2. Then cells were washed twice in PBS and analyzed by flow cytometry. For *ex vivo* experiments (see Fig. 3), thymocytes were stained with Annexin V-APC (BD Biosciences) and 7-amino-actinomycin (7-AAD; Sigma-Aldrich) in binding buffer (0.1 *M* Hepes (pH 7.4); 1.4 *M* NaCl; 25 m*M* $CaCl_2$) during 15 min at room temperature in the dark. At the end of incubation, cells were resuspended in binding buffer and analyzed by flow cytometry.

ROS measurement by DCF fluorescence. Intracellular ROS were measured on isolated thymocytes and MEFs by staining with 10 μmol/l 2′,7′-dichlorofluorescein diacetate (DCF-DA, Sigma-Aldrich) which is oxidized in green fluorescent DCF, as reported previously (7). When specified (see Fig. 5A), thymocytes were co-labeled with DCF-DA and anti-CD4 + anti-CD8 antibodies at 37°C in FACS buffer.

Chemicals for ROS determination and antioxidant assays

Chemicals and enzymes, including 2,6-dichlorophenolindophenol (DCIP), vitamins C and E, glutathione (GSH), ß-cyclodextrin, KH_2PO_4, ethylenediaminetetratraacetic acid (EDTA), diethylenetriaminepentaacetic acid (DTPA), and 2,2,6,6-tetramethylpiperidine-N-oxyl radical (TEMPO) were from Sigma-Aldrich. The spin trap 5-diethoxyphosphoryl-5-methyl-1-pyrroline *N*-oxide (DEPMPO) was synthesized and purified for biological purpose as described in (36).

ROS measurement by electron spin resonance

Measurement of the free radical component of ROS in the blood and thymocytes of irradiated mice was performed by means of spin trapping technique combined with electron spin resonance (ESR) detection. Indeed, spin adducts to a nitrone compound can accumulate to a detectable level due to their relatively long persistency, and generally have characteristic ESR features for a given primary, short-lived free radical. Heparinized blood samples, taken 3 h after whole-body, 6-Gy or 10-Gy irradiation, underwent a quick *in situ* 1:1 mixing in a plastic syringe pre-filled with a cold (5°C) phosphate buffer (40 m*M*) solution of 100 m*M* DEPMPO, 50 m*M* ß-cyclodextrin, and 1 m*M* DTPA, before being placed in a cryotube which was immediately frozen in liquid nitrogen. Inclusion of ß-cyclodextrin within the spin trap solution has been reported to significantly increase the lifetime of DEPMPO spin adducts in reductive milieu such as blood or plasma (Patent : Culcasi M, Pietri S, Tordo P, Gosset G and Karoui H. Method for detecting, identifying and quantifying free radicals, sampling device and kit for ESR. PCT Int. Appl. Application: WO 2007-FR51704 20070720, 2008). Thymocytes obtained from irradiated mice were resuspended in 1 ml PBS containing 20 m*M* of the nitrone DEPMPO, incubated 10 min at room temperature, and centrifuged at 1500 rpm for 5 min. The pellet (thymocytes) and the supernatant were separated, individually placed in cryotubes, and immediately stored in liquid nitrogen.

Each DEPMPO-supplemented sample from irradiated mice was sequentially thawed, placed into a calibrated 50-μl glass capillary (Hirschmann Laborgeräte, Eberstadt, Germany) and scanned at room temperature for its free radical content using a Bruker ESP 300 spectrometer (Karlsruhe, Germany) operating at X-band (9.8 GHz) with a TM-cylindrical cavity and a 100-kHz modulation frequency. ESR acquisition was initiated 60 sec after thawing of the sample by signal averaging of ten 4096-points spectra using the following parameters: microwave power, 10 mW; receiver gain, 1.25×10^5; time constant, 40.96 ms; modulation amplitude, 0.1 G; scan rate, 3.3 G/s for a sweep width of 140 G. ESR signals were quantified by comparing the double integral of simulated spectra (WinSim software, see (12)) to that of 5 μM aqueous TEMPO. Data, which are either directly expressed in μM (blood and supernatant) or first normalized to wet weight (thymocytes), are means of 6–9 independent experiments for each tested group of mice.

Antioxidant activity analysis

Tissue homogenates (100 mg), taken from freshly excised organs carefully rinsed with PBS to remove any blood cells, were homogenized on ice in 0.9 ml of cold MES (GSH + GSSG assay) or 1.15% KCl (ascorbate assay), centrifuged for 15–20 min (10,000 *g*) at 3°C and the supernatants were stored at −80°C. Plasma samples were obtained after blood centrifugation (10,000 *g*) for 15–20 min at 3°C and were stored at −80°C.

Total glutathione levels (reduced (GSH) + oxidized (GSSG) glutathione values) in the supernatants of tissue homogenates were assayed at 404–414 nm (1) in a buffer consisting of 0.4 *M* MES and 1 m*M* EDTA (pH 6), by the glutathione disulfide reductase 5,5′-dithiobis(2-nitrobenzoate) recycling method using a MP96 microplate reader (SAFAS, Monaco). Data are expressed in μmol/g wet weight and represent the mean of 9–18 experiments made en triplicate.

Ascorbate tissue and plasma content was determined according to a spectrophotometric method involving reduction of DCIP dye by ascorbic acid (32). Data are expressed in μmol/g wet weight or in μM for plasma and are the means of 6–18 independent experiments made in triplicate.

Plasma content of vitamin E (α and γ tocopherols) was determined in methanol:water by a HPLC procedure (4) with diode array UV detection at 290 nm (Varian, France). Data are expressed in μM and are the means of at least 6 independent experiments made in triplicate.

GSH and GSSG levels were determined in samples consisting of 5×10^5 thymocytes which were washed twice in ice-cold phosphate buffered saline (pH 7.2). Then 50 m*M* borate buffer (pH 10.5) containing 0.5 % triton was added. An aliquot was removed for protein determination, and remaining protein was precipitated with 1 *M* perchloric acid in 0.2 *M* boric

acid. Samples were centrifuged, and the supernatants (150 μl) were derivatized with 40 m*M* iodoacetic acid at pH 9.0 for 15 min. The pH was adjusted to 9.0 with KOH/tetraborate solution (150 μl). Dansyl chloride was added to give a concentration of 10 m*M*, and samples were left at room temperature for 24 h in the dark to form S-carboxymethyl-N-dansyl-GSH and N,N9-bis-dansyl-GSSG. Unreacted dansyl chloride was removed by chloroform extraction. The GSH and GSSG adducts were separated by HPLC and quantified relative to standards using a fluorescence detector (excitation wavelength, 335 nm; emission wavelength, 515 nm). Chromatographic analysis was performed using a Waters Alliance^{TM} System (Milford, MA) equipped with a Waters 2690 XE separation module and a Waters 474 Scanning fluorescence detector controlled by the Waters Millenium^{TM} Chromatography manager software. Separation is achieved at room temperature on a 3-aminopropyl column (250 mm × 4.6 mm; 5 μm; Macherey–Nagel, Düren, Germany) with an isocratic flow rate of 1.2 mL.min^{-1}. Solvent A is a 0.2 *M* acetate buffer (pH 4.6) and solvent B is 80% (v/v) methanol/water. Quantification was based on peak area.

Western blot analysis

MEFs were plated as reported above, and lysed 24 hours after irradiation in lysis buffer (50 m*M* Hepes, 150 m*M* NaCl, 1 m*M* EDTA, 1 m*M* EGTA, 10% glycerol, 1% triton X-100, 25 m*M* NaF, 10 μ*M* $ZnCl_2$, protease inhibitors cocktail (Sigma-Aldrich), 1 m*M* Na_3VO_4). Samples were centrifuged at 16,000 *g* for 10 min at 4°C. Cleared lysates with adjusted protein concentration were used for Western blot analysis. Samples were mixed with Laemli buffer (125 m*M* Tris/HCl, 288 m*M* β-mercaptoethanol, 20% glycerol, 9% SDS, 4.5 mg/ml bromophenol blue) and boiled for 5 min. Total cellular protein (100 μg/lane) were separated by SDS-polyacrylamide gel electrophoresis, transferred onto nitrocellulose membrane, then Western blot was probed with the following antibodies: purified mouse anti-p62 Lck ligand (BD Transduction Laboratories) and mouse monoclonal anti-vinculin. Visualization of the proteins was performed using enhanced chemiluminescence reagent (Millipore, Billerica, MA) on the Fusion FX7 device (Fisher Bioblock Scientific, Illkirch, France). Equal protein loading was confirmed by probing membranes with antibodies against vinculin. See Supplementary Data.

Statistical analysis

Data are expressed as means ± standard error (SE). Differences were analyzed by one-way analysis of variance followed by Duncan test or unpaired Student's *t* test and were considered to be significant at $p < 0.05$.

Results

TP53INP1 expression is augmented in thymocytes upon stress-induced cell death

To address whether and how TP53INP1 influences cell death, we used TP53INP1-deficient mice generated in the laboratory (16) and backcrossed on C57BL/6 parental genetic background for nine generations. We focused our analysis on the thymus for two reasons: (i) TP53INP1, that we initially named Thymus-Expressed Acidic Protein (TEAP), is highly expressed in thymus (8), and (ii) the thymus is well suited for apoptosis analysis because a high number of thymocytes die during their maturation through positive and negative selection (19, 33). We first checked that TP53INP1 expression is increased in the thymus of wild-type (WT) mice upon *in vivo* treatment by cell-death inducers [*i.e.*, whole-body gamma-irradiation (6-Gy) or dexamethasome (corticoid analog) intraperitoneal injection (200 μg)]. Figure 1A shows that expression of TP53INP1 is significantly induced in thymocytes 6 h after irradiation or dexamethasone treatment. A time course experiment showed that TP53INP1 expression levels peaked 6 h after irradiation (not shown). This result suggests that TP53INP1 certainly plays a role during stress response in the thymus.

In vivo *radiation- and dexamethasone-induced cell death is increased in thymocytes in the absence of TP53INP1*

We assessed thymocyte death by flow cytometry analysis using anti-CD4- and anti-CD8 antibodies. The CD4+CD8+ (double-positive, DP) thymocytes are the predominant immature cell type in the thymus, and the critical stage at which T cell selection takes place, as such DP cells are highly sensitive to radiation- and dexamethasone-induced death (2, 14, 39). We analyzed thymic cell death induced by whole-body irradiation (6 Gy), and observed that the percentage of DP cells is considerably decreased 24 h after irradiation (Fig. 1B), and more drastically in TP53INP1-deficient mice compared to WT (0.9% deficient versus 6.7% WT DP cells). We also analyzed glucocorticoid-induced thymocyte death by dexamethasome intraperitoneal injection (200 μg), and observed a higher decrease of DP cells percentage in TP53INP1-deficient mice compared to WT (2.6% deficient versus 6.4% WT DP cells). This higher mortality of TP53INP1-deficient DP thymocytes is also observed after 2 Gy whole-body irradiation and 150 μg dexamethasome injection (data not shown). These data show that TP53INP1-deficient DP thymocytes are more sensitive than WT to induced-cell death. Interestingly, it is known that dexamethasome-induced cell death is independent of p53 contrary to radiation-induced cell death which is impaired in p53-deficient thymocytes (10, 25). Thus TP53INP1 absence confers cell death sensitivity in both p53-dependent and -independent settings.

In vivo *radiation-induced cell death in the absence of TP53INP1 is apoptosis*

We addressed whether TP53INP1-deficient thymocytes die by apoptosis upon stress. To this aim, we analyzed thymocytes 3 h after whole-body irradiation, considering four features of apoptosis (*i.e.*, reduction of cell size, loss of mitochondrial membrane potential, caspases activation, and DNA fragmentation). All these events were analyzed by flow cytometry. We underlined the live cells region (R1) and the dying cells (reduced size) region (R2) on the FSC/SSC dot-blot (Fig. 2A). This analysis shows that the percentage of dying cells with reduced size is increased in TP53INP1-deficient thymus compared to WT. In addition, we used the $DiOC_6$ fluorescent marker to quantify mitochondrial membrane potential loss, and measured the percentage of $DiOC_6$-negative cells corresponding to dying cells. This percentage is higher in TP53INP1-deficient thymocytes compared to WT (Fig. 2B). In the same manner, the percentage of cells in which caspases are activated is higher in

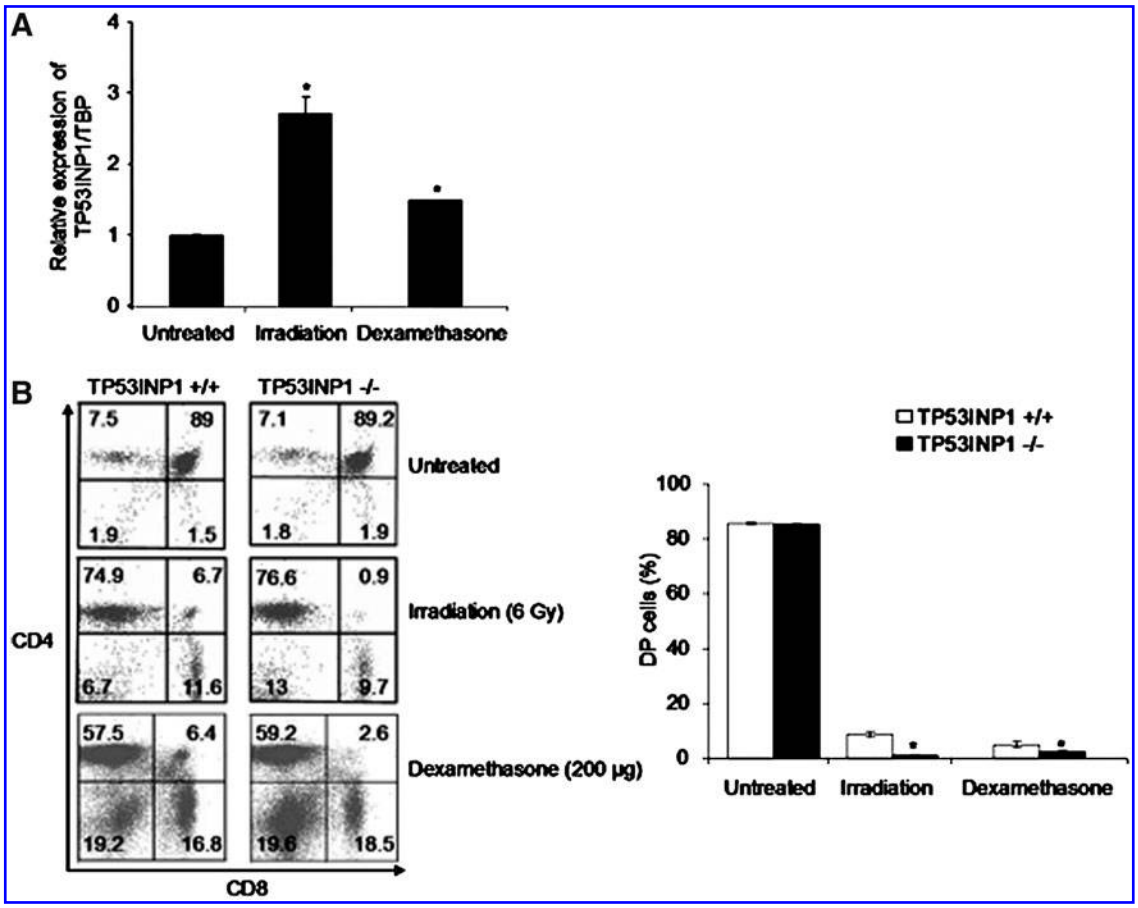

FIG. 1. TP53INP1 is involved in thymocytes death *in vivo*. (A) TP53INP1 expression is increased in thymocytes upon *in vivo* induced stress. Histogram shows relative TP53INP1 expression quantified by qRT-PCR in thymocytes derived from C57BL/6 mice ($n=3$ for each conditions) 6 h after whole-body irradiation (6 Gy) or intraperitoneal injection of dexamethasone (200 μg). Data are represented as means of triplicate ± SE. *$p<0.05$ compared to control. Data are representative of three independent experiments. **(B)** *In vivo* thymocytes death is increased in the absence of TP53INP1. TP53INP1 +/+ and TP53INP1-/- mice were irradiated or injected with dexamethasone ($n=3$ for each genotype in each condition). Twenty-four hours later, thymocytes were stained with CD4 and CD8 antibodies and analyzed by flow cytometry. Dot plots show percentage of different subpopulations (CD4-8-; CD4+8+ (DP); CD4+ and CD8+ cells) in each quadrant. Histogram (*right*) shows quantification of DP cells percentage. As both stresses induce preferential cell death of DP cells, percentage of DP cells decreases upon stress, leading to relative increase of all other subpopulations percentage. *$p<0.05$ compared to +/+. Dot plots are representative of three independent experiments.

the absence of TP53INP1 (Fig. 2C). Finally, lack of TP53INP1 is correlated with increased DNA fragmentation after irradiation as evidenced by the higher percentage of permeabilized PI-labeled cells in the subG1 region of histogram in deficient cells (Fig. 2D). These apoptosis-associated features were also assessed in the *in vivo* dexamethasome-induced cell death setting, with the same observations as irradiation (data not shown). Altogether these data clearly show that upon stress, the percentage of cells committed in apoptosis is higher in the absence of TP53INP1.

Ex vivo *apoptosis of thymocytes is also increased in the absence of TP53INP1*

We then addressed the question of whether increased sensitivity of TP53INP1-deficient thymocytes to induced-death is intrinsic to thymocytes or dependent on their microenvironnement (stromal cells) in the thymus. Indeed, lympho–stromal interactions play a crucial role in T-cell development and selection (23, 30, 40). For that purpose, we analyzed thymocytes *ex vivo* after 24 h and 48 h in culture, both by cell counting and Annexin V labeling revealing phosphatidylserine (PS) translocation to the outer leaflet of the plasma membrane (also a hallmark of apoptosis). In culture, thymocytes die spontaneously because of lack of survival signals delivered by stromal cells. This spontaneous death is increased in the absence of TP53INP1 (Fig. 3A). Notably, at 48 h, we detected mostly late apoptotic cells (7-AAD+) with a higher percentage of these cells in deficient thymocytes compared to WT. Both irradiation (Fig. 3B) and dexamethasone treatment (Fig. 3C) accelerate cell death as shown by predominance of late apoptotic cells as soon as 24 h after treatment, again with a higher percentage of these cells in deficient thymocytes compared to WT. We can conclude that TP53INP1 deficiency increases thymocytes (spontaneous and stress-induced) cell death *ex vivo* as observed *in vivo*. Therefore higher sensitivity to cell death is an intrinsic property of TP53INP1-deficient thymocytes.

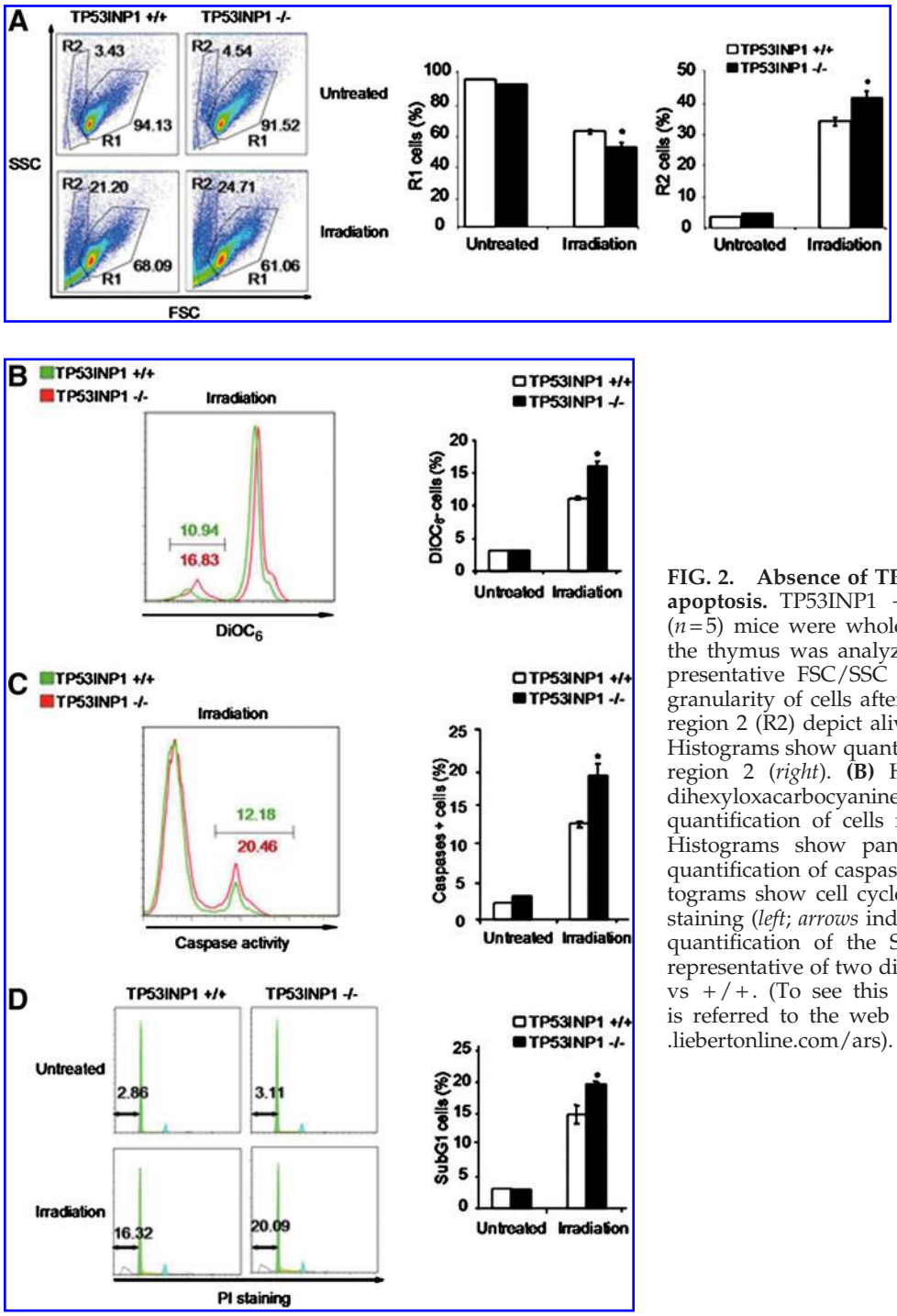

FIG. 2. Absence of TP53INP1 increases cell death by apoptosis. TP53INP1 +/+ ($n=5$) and TP53INP1 -/- ($n=5$) mice were whole-body irradiated, and 3 h later the thymus was analyzed by flow cytometry. **(A)** Representative FSC/SSC dot plot (*left*) shows size and granularity of cells after irradiation. Region 1 (R1) and region 2 (R2) depict alive and dying cells, respectively. Histograms show quantification of region 1 (*middle*) and region 2 (*right*). **(B)** Histograms show $DiOC_6$ (3,3'-dihexyloxacarbocyanine iodide) staining (*left*) and quantification of cells negative for $DiOC_6$ (*right*). **(C)** Histograms show pan-caspases activation (*left*) and quantification of caspases positive cells (*right*). **(D)** Histograms show cell cycle analysis by propidium iodide staining (*left*; *arrows* indicate the SubG1 region) and the quantification of the SubG1 region (*right*). Data are representative of two different experiments. $^*p<0.05$ -/- vs +/+. (To see this illustration in color the reader is referred to the web version of this article at www.liebertonline.com/ars).

TP53INP1 deficiency does not overcome impaired radiation-induced apoptosis of p53-deficient thymocytes

Radiation-induced cell death of p53-deficient thymocytes was reported to be impaired (10, 25). In that context, we assessed whether higher sensitivity of TP53INP1-deficient thymocytes to cell death could also be observed on a p53-deficient background. To this aim, we irradiated double-deficient (TP53INP1 -/- p53 -/-) mice and evaluated cell death in the thymus of these mice compared with p53 single-deficient mice (Fig. 4). As expected, the percentage of DP thymocytes is not decreased in p53-deficient mice 24 h after irradiation. Nevertheless, this percentage is reduced in p53-deficient mice 48 h after irradiation, meaning that radiation-induced cell death of p53-deficient thymocytes is not completely impaired but rather delayed. Interestingly, TP53INP1 deficiency does not accelerate the delayed death of p53-deficient thymocytes. Similarly, in the *ex vivo* thymocytes cell death setting, TP53INP1 deficiency does not accelerate death of p53-deficient thymocytes (data not shown). Altogether, these data suggest that resistance to apoptosis in the absence of p53 is

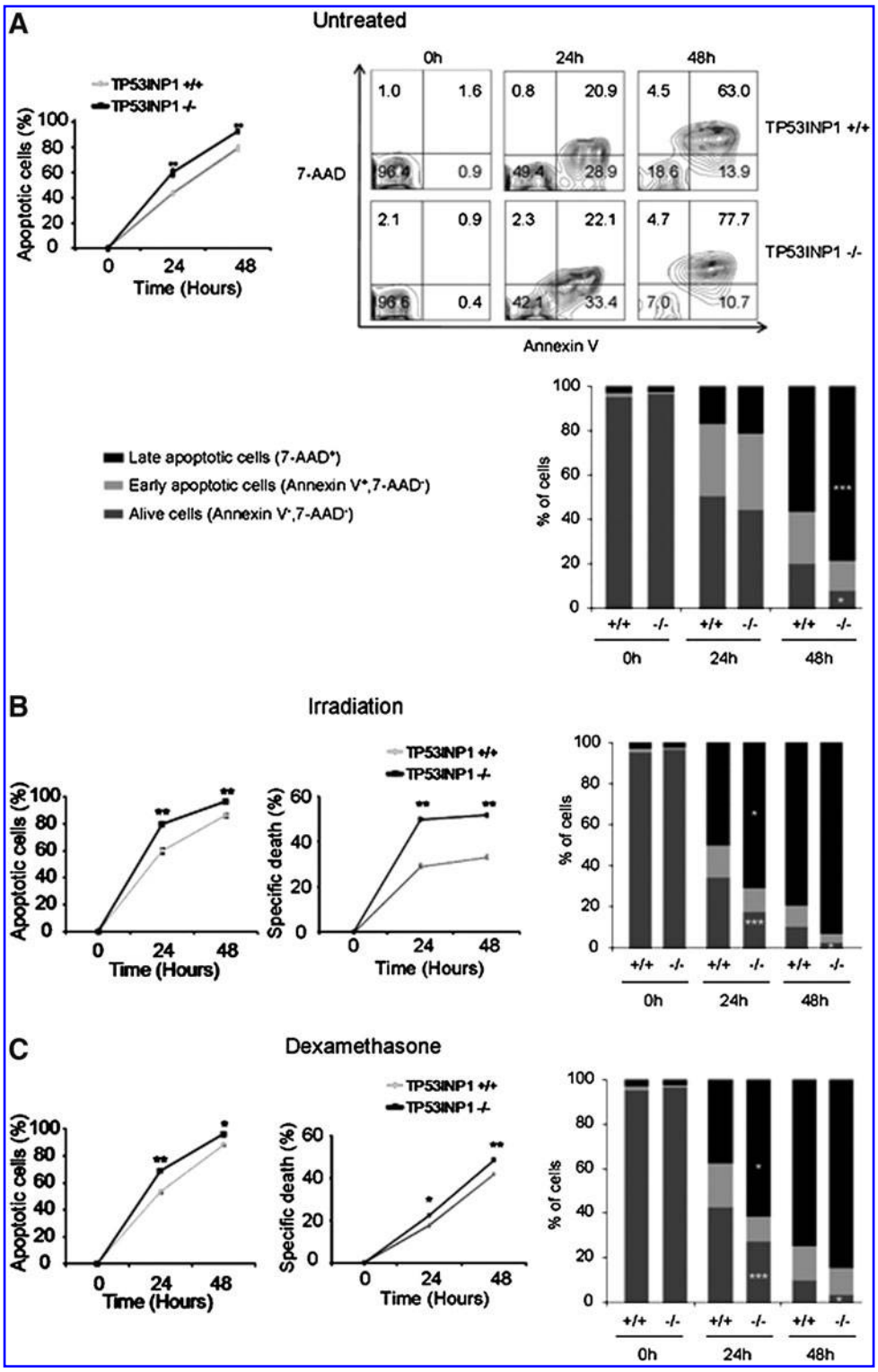

FIG. 3. Absence of TP53INP1 increases thymocytes cell death *ex vivo*. Thymocytes derived from TP53INP1 +/+ ($n=3$) and TP53INP1 -/- ($n=3$) mice were cultivated *ex vivo* (spontaneous death, **A**), exposed to irradiation (0.5 Gy, **B**) or cultured in presence of dexamethasone treatment (10^{-9} *M*, **C**). The percentage of apoptotic cells was determined by two kinds of methods: (*left*) Analysis of FSC/SSC dot-blot as shown on Figure 2A permits to quantify live cells (R1 region). The formula to calculate dead cell is (100 - (alive cell/total cells)). Specific cell death induced by stimuli was calculated by the following equation (induced apoptosis - spontaneous cell death)/(100 - spontaneous cell death)×100. (*right*) Annexin V and 7-AAD staining followed by flow cytometry analysis. Histograms show quantification of each population in AnnexinV/7-AAD staining. Representative dot-plots are shown only in the case of untreated cells. Data are representative of three different experiments. *$p<0.05$, **$p<0.01$, and ***$p<0.005$ (-/- vs +/+).

dominant over apoptosis sensitivity in the absence of TP53INP1.

We previously reported that, upon oxidant challenge, expression of p53 targets Puma and Bax is decreased in TP53INP1 -/- compared to TP53INP1 +/+ MEFs (7). We investigated in thymocytes the expression of p53 pro-apoptotic targets Bax, Puma, Bim, and Noxa (Supplementary Fig. S1A) and observed a comparable level of induction of these genes upon irradiation in TP53INP1 -/- and TP53INP1 +/+ thymocytes (Noxa is even less expressed in TP53INP1 -/- thymocytes). Moreover, we evaluated BAX protein level by Western blotting (Supplementary Fig. S1B), and observed that BAX level increases in irradiated TP53INP1 +/+ thymocytes contrary to TP53INP1 -/- thymocytes where it is poorly

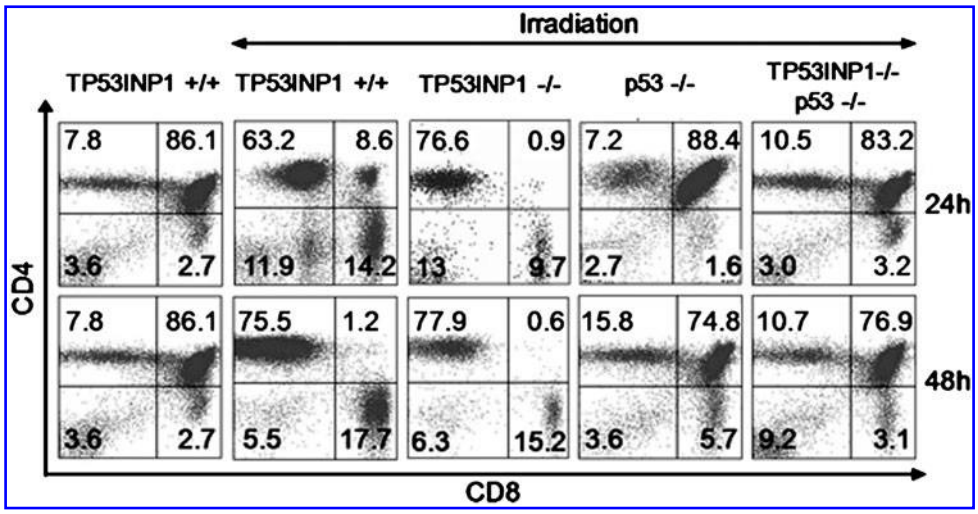

FIG. 4. Absence of TP53INP1 does not affect thymocytes resistance to cell death on a p53-deficient background. Cohort of TP53INP1 + / +, TP53INP1-/-, p53-deficient mice, and double p53-TP53INP1-deficient mice were irradiated, and 24 or 48 h later thymocytes were stained with anti-CD4 and anti-CD8 antibodies and analyzed by flow cytometry ($n = 3$ for each genotype and each time frame). Representative dot plots of stained thymocytes show the percentage of CD4-8-, CD4 + 8 +, CD4 +, and CD8 + cells. The nonirradiated control is shown solely in the case of TP53INP1 + / + mice since the CD4/CD8 dot plot does not differ between genotypes. Data are representative of three independent experiments.

increased. Altogether these data suggest that the higher sensitivity to induced cell death observed in the absence of TP53INP1 does not depend on the transcriptional activity of p53 on its pro-apoptotic target genes.

Oxidative stress is exacerbated in TP53INP1-deficient thymocytes in vivo

To investigate the role of oxidant stress and ROS formation in the higher sensitivity to cell death of irradiated TP53INP1-deficient *vs*. WT thymocytes, we stained thymocytes 3 h after whole-body irradiation (6-Gy) with DCF-diacetate that freely penetrates cells and generates fluorescent DCF upon oxidation, constituting an intracellular marker of cell oxidant stress. We co-labeled thymocytes with anti-CD4 and anti-CD8 antibodies in order to measure ROS level in the different thymocytes subpopulations. DCF mean fluorescence intensity (MFI) does not differ between WT and deficient total thymocytes as reported previously (7), despite a faint but significant MFI increase observed in deficient SP (CD4 + or CD8 +) subpopulations (Fig. 5A). By contrast, MFI is significantly higher in all irradiated thymocytes subpopulations deficient for TP53INP1 compared to WT (Fig. 5A), showing that cell oxidant stress is exacerbated in thymocytes lacking TP53INP1.

In an attempt to address the mechanisms responsible for the global irradiation-induced oxidant stress seen in Figure 5A, we used ESR spectrometry to examine free radical production in blood and thymocytes from irradiated mice of both groups. A baseline response is expected in WT animals because a portion of the damage sustained by cells exposed to ionizing radiation is associated with primary formation of hydroxyl radicals ($HO^{\cdot}$) along with hydrated electrons (e^{-}_{aq}) and hydrogen atoms ($H^{\cdot}$) during radiolysis of water (6). To minimize interference of the spin trap DEPMPO with biologically-unrelated radiolytic free radicals, the spin trap was incubated *ex vivo* with blood or thymocytes taken from whole-body irradiated animals 3 h after irradiation. Under these conditions, all samples from non-irradiated animals were diamagnetic (*i.e.*, no paramagnetic detection of ROS) while those from irradiated mice yielded weak signals characteristic of mixture of DEPMPO spin adducts, the general structure and a typical example of which are shown in Figure 5B in the case of a 6-Gy dose. Good fits with experimental spectra are obtained by computer simulation assuming a mixture of DEPMPO/$^{\cdot}$OH adduct (DEPMPO-OH, as a ~55:45 mixture of *trans* ($a_N = 14.0$ G, $a_H = 12.8$ G, and $a_P = 47.4$ G):*cis* diastereoisomers ($a_N = 14.0$ G, $a_H = 14.3$ G, and $a_P = 47.4$ G); see (11)), DEPMPO-H (($a_N = 15.5$ G, $a_{H1} = 14.3$ G, $a_{H2} = 14.7$ G, and $a_P = 56.2$ G; see(3)) and a minor, unidentified species DEPMPO-R ($a_N = 15.0$ G, $a_H = 14.6$ G, and $a_P = 49.3$ G). With respect to WT mice, the total ESR signal in TP53INP1-deficient animals is more significantly increased in blood and thymocytes pellets (~2–2.5 times) than in supernatant of thymocytes incubation, although intergroup difference in the latter is still significant (Fig. 5B).

The above evidence of an irradiation-related DEPMPO adduct formation prompted us to investigate the effect of increasing radiation dose on the DEPMPO-H component of the ESR signal, in relation with e^{-}_{aq} and $H^{\cdot}$ formation during water radiolysis. Therefore animals from both groups ($n = 4$) were submitted to the same irradiation and sampling protocol for ESR, except that dose was 10 Gy instead of 6 Gy. Compared to 6-Gy-irradiated animals, the mean percentage of DEPMPO-H in the total ESR signal is similarly and significantly increased ($p < 0.05$) in the blood of WT (53% *vs*. 66%) and TP53INP1 -/- (58% *vs*. 69%) 10-Gy irradiated animals, although the total DEPMPO spin adduct concentrations are not significantly affected (data not shown). Since the same trend is also observed when DEPMPO-H signals were recorded in the supernatant and pellets of thymocytes, this component of the total ESR signal appears radiation-dependent.

Increased apoptosis parallels exacerbated oxidative stress in TP53INP1-deficient thymocytes ex vivo

We postulated that increased ROS level in TP53INP1-deficient cells could be involved in their increased sensitivity to induced cell death. We assessed this hypothesis in the *ex vivo* experimental setting by supplementation with the antioxidant NAC in the culture medium. Spontaneous and radiation-induced cell death was quantified by Annexin V and 7-AAD labeling. As expected, NAC treatment reduces ROS level

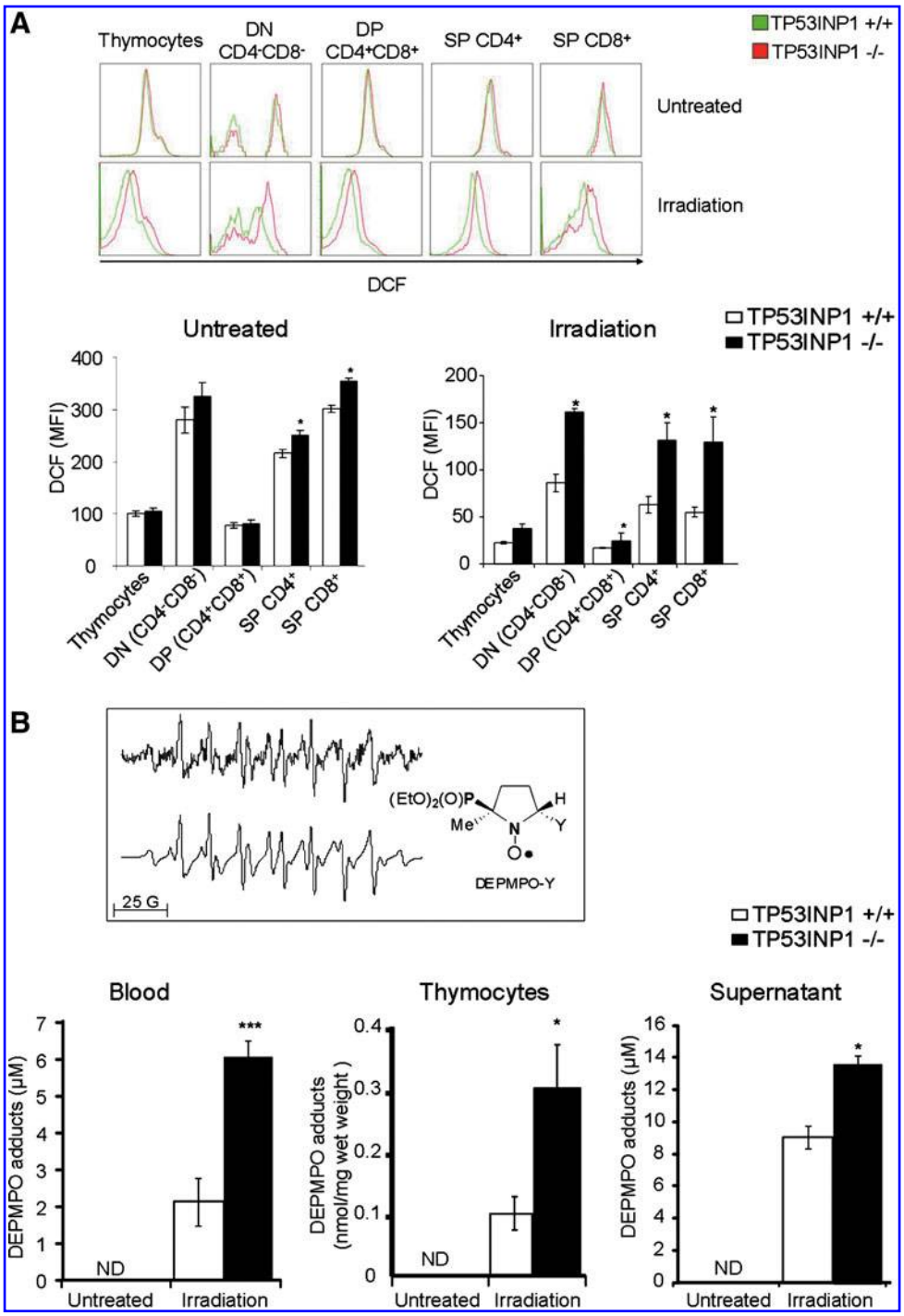

FIG. 5. Absence of TP53INP1 increases ROS production upon induced stress. (A) TP53INP1 +/+ and TP53INP1 -/- mice ($n=2$ in each group) underwent a 6-Gy irradiation; 3 h later thymocytes were co-stained by dichlorofluorescein diacetate (DCF) and anti-CD4+ anti-CD8 antibodies, and analyzed by flow cytometry. (*upper*) Representative histograms of DCF staining. (*lower*) Quantification of DCF mean fluorescence intensity (MFI) in total thymocytes and in each subpopulation of thymocytes. $*p<0.05$ *vs.* TP53INP1 +/+ group. **(B)** *Insert*: typical ESR spectrum (*upper trace*) recorded in the DEPMPO-supplemented blood of a 6-Gy-irradiated TP53INP1 -/- mouse. The spin trap (0.1 *M*) was added in the blood taken 3 h after irradiation and simulation of the signal (*lower trace*) indicated a mixture of DEPMPO-H (63%), DEPMPO-OH (28%), and DEPMPO-R (9%). In the general formula of DEPMPO-Y, the *trans* isomer is represented and coupling nuclei are indicated in **bold**. Histograms show the mean total levels of DEPMPO spin adducts obtained in tested samples. Statistics: $*p<0.05$ and $***p<0.001$ *vs.* TP53INP1 +/+ group ($n=9$ in each group). No detectable (ND) ESR signals were seen in both groups when samples were obtained from control, nonirradiated animals (untreated). (To see this illustration in color the reader is referred to the web version of this article at www.liebertonline.com/ars).

(Fig. 6A), as well as cell death (Fig. 6B), both in untreated and irradiated thymocytes. Most importantly, NAC abolishes differences of ROS level between TP53INP1-deficient and WT thymocytes (Fig. 6A). Moreover, NAC treatment strongly reduces the cell death difference between TP53INP1-deficient and WT thymocytes, this reduction being apparent mostly for late apoptotic cells (Fig. 6B). This crucial result suggests that higher cell death sensitivity of TP53INP1-deficient thymocytes is linked to their higher content of ROS.

Radiation-induced apoptosis is also increased in fibroblasts in the absence of TP53INP1, which is related to ROS increase

We sought to demonstrate that cell-death sensitivity in the absence of TP53INP1 is not restricted to thymocytes. We therefore investigated cell-death in MEFs transformed by overexpression of E1A and Ras^{V12} oncogenes. Cell death was induced by gamma-irradiation (10 Gy), and quantified by PI

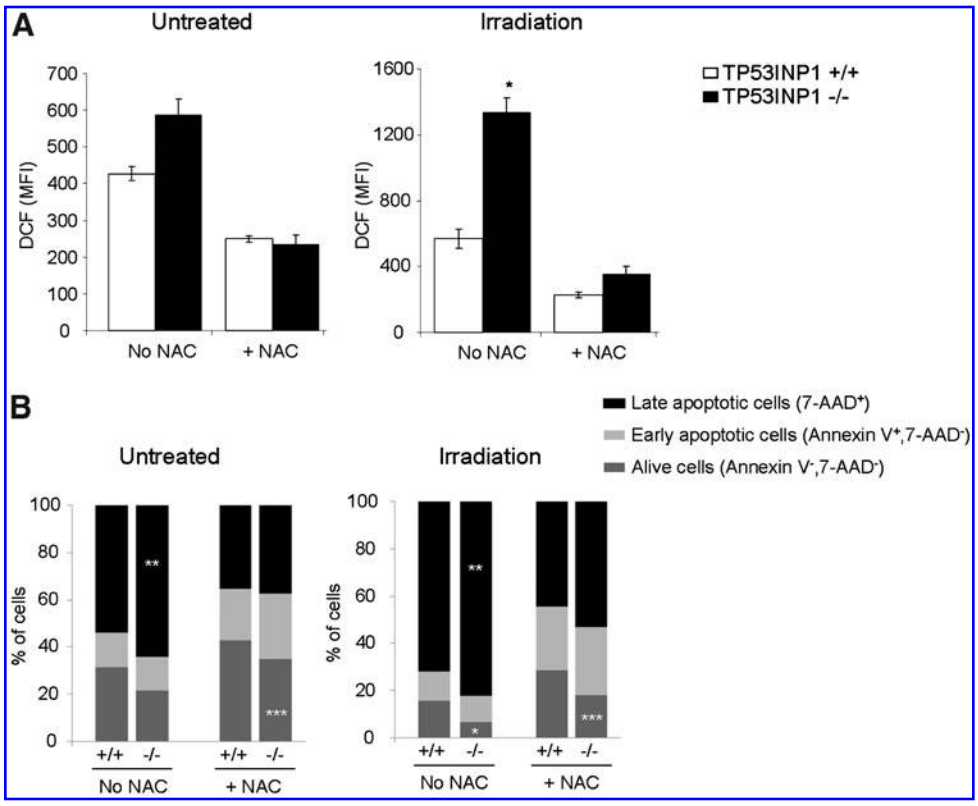

FIG. 6. Antioxidant NAC treatment abolishes both ROS level and cell death sensitivity differences between TP53INP1-deficient and WT mice. Thymocytes of each genotype (TP53INP1 +/+ and TP53INP1 -/-) were cultivated (*ex vivo* setting) in the absence (no NAC) or in the presence (+NAC) of NAC (*N*-acetylcysteine, 20 m*M*), and cell death was measured 48 hours later. This experiment was done in parallel with *ex vivo*-irradiated thymocytes. **(A)** Histograms show MFI (Mean Fluorescence Intensity) of DCF measured by flow cytometry in triplicate for each mouse. $N=6$ in each group. **(B)** Histograms show quantification of Annexin V and 7-AAD staining. Data are representative of two independent experiments. $^{*}p<0.05$, $^{**}p<0.01$, and $^{***}p<0.005$ (-/- vs +/+).

labeling and caspases activation assay. As observed for thymocytes, radiation-induced death is higher in TP53INP1-deficient fibroblasts compared to WT (Figs. 7A and 7B). We tested the effect of antioxidant by supplementation with NAC in the culture medium. We observed that NAC treatment significantly reduces ROS level in both genotypes (Fig. 7C). In addition, NAC completely abolishes cell death difference between WT and TP53INP1-deficient fibroblasts (Figs. 7A and 7B). Altogether, these results show that TP53INP1-deficient fibroblasts are more sensitive to induced cell death than WT, and that their abnormal high ROS content is responsible of their higher sensitivity to stress-induced cell death.

Antioxidant defenses are defective in the absence of TP53INP1

We previously reported decreased level of ascorbate (vitamin C) in the blood of TP53INP1-deficient mice (on a mixed genetic background) (16), suggesting a link between reduced antioxidant defenses and deregulated redox status in the absence of TP53INP1. We confirm here that blood of TP53INP1-deficient mice (on C57BL/6 genetic background) is strongly depleted in ascorbate, and further show that it is also depleted in vitamin E (Fig. 8A). Furthermore, we show that level of ascorbate (vitamin C) is two-fold reduced in thymocytes of

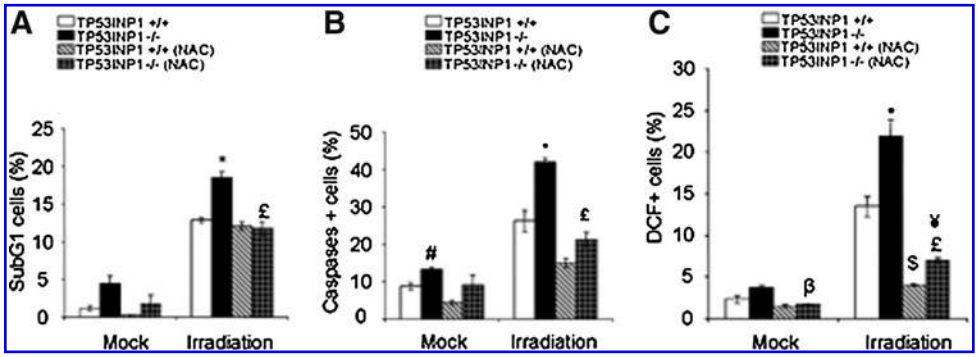

FIG. 7. Absence of TP53INP1 increases ROS-driven death of transformed MEFs *in vitro*. Transformed MEFs of each genotype (TP53INP1 +/+ and TP53INP1 -/-) were cultivated in the presence or absence of 20 m*M* NAC and were irradiated at 10 Gy. Histograms show quantification of cells in SubG1 region of PI staining **(A)**, caspases positive cells **(B)**, and ROS level **(C)**, measured by flow cytometry. Data are means of triplicate ± SE and are representative of two different experiments. $p<0.05$: *TP53INP1 -/- versus TP53INP1 +/+, # mock TP53INP1 -/- versus mock TP53INP1 +/+, $ NAC-treated TP53INP1 +/+ versus TP53INP1 +/+, £ NAC-treated TP53INP1 -/- versus TP53INP1 -/-, ¥ NAC-treated TP53INP1 +/+ versus NAC-treated TP53INP1 -/-. β represents $p<0.005$ NAC-treated mock TP53INP1 -/- versus mock TP53INP1 -/-.

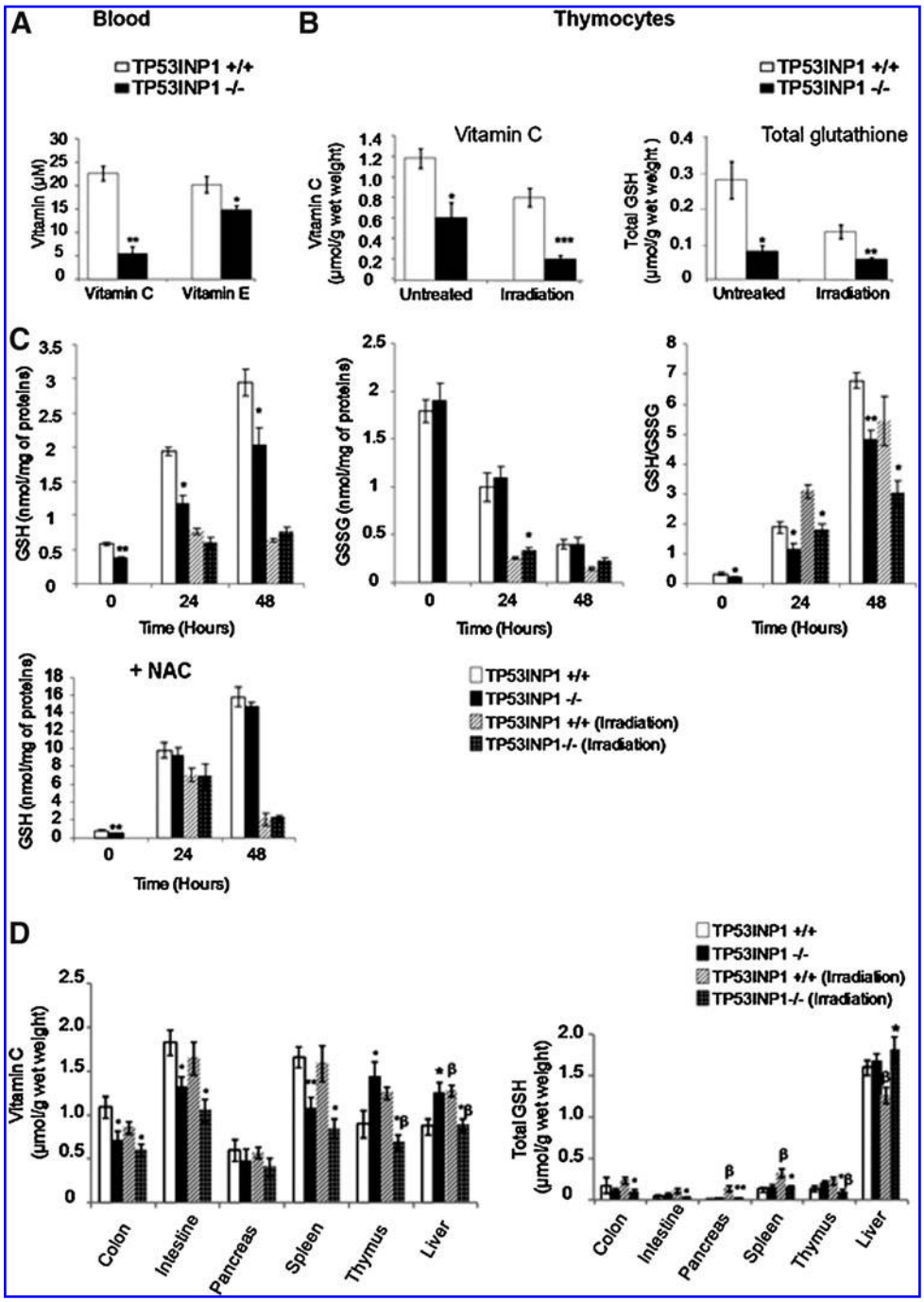

FIG. 8. Absence of TP53INP1 decreases antioxidant level. (A) Histogram shows antioxidants level (vitamins C and E) in the blood of mice deficient or not for TP53INP1. $*p<0.05$ vs TP53INP1 +/+ group ($n=6$ in each group). **(B)** TP53INP1 +/+ ($n=9$) and TP53INP1 -/- ($n=9$) mice were whole-body irradiated (6 Gy); 3 hours later, antioxidants level (vitamin C and total glutathione) were measured in thymocytes. $*p<0.05$, $**p<0.01$, and $***p<0.001$ *vs.* TP53INP1 +/+ group. **(C)** Dosage of reduced (GSH) and oxidized glutathione (GSSG) in thymocytes *ex vivo*. Thymocytes derived from TP53INP1 +/+ ($n=4$) and TP53INP1 -/- ($n=4$) mice were cultivated and exposed to irradiation (0.5 Gy) or not (spontaneous death), in the presence or not of NAC (20 m*M*). GSH and GSSG cell levels were determined at 0, 24, and 48 h of culture, and the ratio GSH/GSSG was determined. $*p<0.05$, $**p<0.01$. Note that in the presence of NAC, high levels of GSH are observed whereas no GSSG was detectable. **(D)** Mice were whole-body irradiated or not, and 3 h later vitamin C and total glutathione levels were measured in different organs. $*p<0.05$, $**p<0.01$ correspond to TP53INP1 -/- versus TP53INP1 +/+ and β represents irradiated group compared to nonirradiated. $N=5$ for nonirradiated mice of both groups. $N=13$ and $n=9$, respectively, for irradiated TP53INP1 +/+ and TP53INP1 -/- mice.

TP53INP1-deficient mice compared to WT (Fig. 8B, left). Upon irradiation, ascorbate level drops more severely in TP53INP1-deficient thymocytes compared to WT. We observed also a depletion of total glutathione in TP53INP1-deficient thymocytes compared to WT at basal level and upon irradiation (Fig. 8B, right). Next, we determined reduced (GSH) and oxidized (GSSG) glutathione levels and the GSH/GSSG ratio in thymocytes at different times in culture, irradiated or not, with or without NAC complementation (Fig. 8C). We observe a GSH steady-state defect in TP53INP1-deficient thymocytes, and a higher level of GSSG at 24 h in irradiated deficient thymocytes compared to WT. Most importantly, in each situation, the GSH/GSSG ratio is significantly lower in TP53INP1-deficient cells compared to WT. Following complementation with NAC, which is a precursor of glutathione, GSH level is highly increased and GSSG is undetectable, independently of the genotype. Altogether, these data show that loss of glutathione in TP53INP1-/- cells is a critical factor in sensitizing these cells to oxidative stress.

We further investigated ascorbate and glutathione levels in different organs of TP53INP1-deficient mice compared to WT. Figure 8D shows that ascorbate level is reduced in organs of TP53INP1-deficient mice compared to WT, with the exception of pancreas (no difference) and thymus and liver where

ascorbate level is higher in deficient mice compared to WT. Interestingly, upon irradiation, ascorbate level increases significantly in WT thymus and liver, whereas it drops in other TP53INP1-deficient organs. By contrast, glutathione level does not differ in all tested organs of TP53INP1-deficient mice compared to WT in basal state (Fig. 8D). Nonetheless, glutathione level fluctuations are observed upon irradiation in organs of WT mice (increase in the spleen or decrease in the liver) but are not observed in deficient organs except in thymus.

Collectively, these data show that small molecule antioxidant defenses are unbalanced in the absence of TP53INP1.

Autophagy is impaired in the absence of TP53INP1

Antioxidants defects in TP53INP1-deficient mice suggest reduced protection against induced cell death in the absence of TP53INP1. Since autophagy is an essential pro-survival cell process (24), we wondered whether this process occurs normally in TP53INP1-deficient cells. To assess this question, we investigated the protein level of p62/SQSTM1 autophagy effector which is an adaptor involved in the elimination of polyubiquinated protein aggregates by autophagy. Monitoring the level of p62 is one of the primary methods to evaluate autophagy, since this level decreases during the course of autophagy. In consequence accumulation of p62 is a hallmark of autophagy-defective cells (28, 29). We observed that the basal level of p62 is higher in TP53INP1-deficient MEFs than in WT (Fig. 9), suggesting impaired autophagy in the absence of TP53INP1. Moreover, level of p62 is not significantly reduced in WT MEFs upon irradiation, differing from TP53INP1-deficient MEFs where p62 level is increased. These data suggest that autophagy which confers protection against stress is impaired in TP53INP1-deficient cells.

Discussion

We report here that the stress protein TP53INP1 plays a protective role in the thymus. Indeed, expression of TP53INP1 is increased in thymocytes upon *in vivo* whole-body radiation and glucocorticoid exposure, as observed in every *in vitro* stress settings reported to date and *in vivo* in inflamed organs (13, 22, 31, 44). Furthermore, we show here that lack of TP53INP1 exacerbates thymocytes sensitivity to induced apoptosis. In addition, increased sensitivity to induced cell death in the absence of TP53INP1 is not cell-type dependent since it is also observed in embryonic fibroblasts. These observations are astonishing because we previously reported a pro-apoptotic role of TP53INP1 in ectopic overexpression settings (44) which appeared consistent with its anti-tumoral function (15). Therefore, our prediction was that TP53INP1-deficiency would impair apoptosis. In contrast to this prediction, this study indicates that deficiency in TP53INP1 extends the sensitivity of cells to stress-induced death. We provide compelling evidence for this result by analyzing induced cell death in different cell types [*i.e.*, immune cells during development (thymocytes), transformed fibroblasts and primary fibroblasts (not shown)].

Hence, we propose a model to reconcile these two apparently opposite functions of TP53INP1 (Fig. 10). Stress response involves high expression of TP53INP1 which participates either in cell cycle arrest permitting damage repair or in cell death depending on stress duration and intensity (Fig. 10, top). In the absence of TP53INP1 in deficient mice (Fig. 10, bottom), participation of TP53INP1 in stress resolution is lacking, which favors cell elimination by apoptosis. As TP53INP1 is lost in several types of human tumors (15, 21), we postulate that not only its anti-proliferative activity is missing (which is consistent with its anti-tumoral function) but also that apoptosis of cells is favored (which could be counterintuitive for an anti-tumoral function). Nevertheless, in some settings, increased apoptosis has been reported to favor tumorigenesis by promoting regenerative proliferation (26). This issue is currently under investigation in the laboratory.

Interestingly, TP53INP1 absence confers increased thymocyte death sensitivity in both p53-dependent and independent settings. Indeed, this sensitivity is observed both in the setting of p53-dependent cell death (irradiation, and etoposide treatment; data not shown) and p53-independent cell death (dexamethasome). Consistently, this sensitivity does not rely on increased expression of pro-apoptotic targets of p53, since quantitative RT-PCR experiments show similar level of expression of Bax, Puma, Noxa, and Bim in thymocytes of both genotypes, which is reminiscent of previously reported impaired induction of Bax and Puma expression upon stress in TP53INP1-deficient MEFs (7). For those reasons, we propose that death sensitivity in the absence of TP53INP1 does not exclusively depend on p53 transcriptional activity.

The mechanism of increased sensitivity to death in the absence of TP53INP1 was provided by the evidence of a correlation between ROS increase and cell death increase in the absence of TP53INP1. Indeed, treatment with an antioxidant (NAC) abrogates the difference of cell death induction between TP53INP1-deficient and WT cells (thymocytes as well as MEFs), demonstrating that increased sensitivity to cell

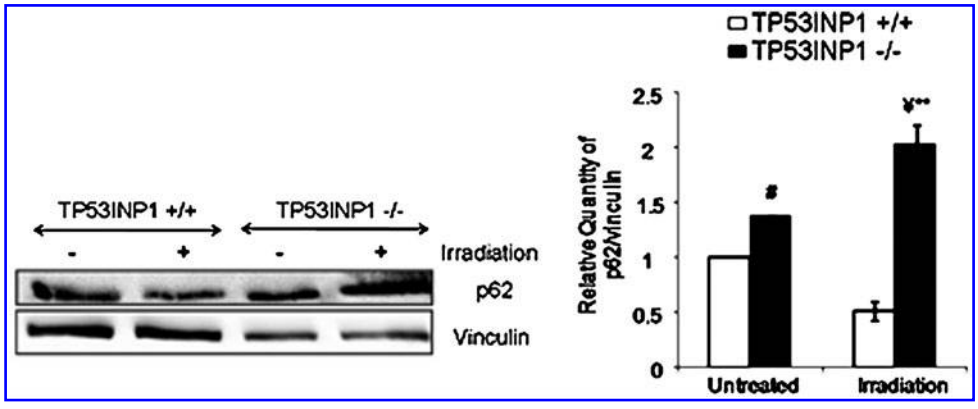

FIG. 9. Absence of TP53INP1 decreases autophagy in transformed MEFs *in vitro*. Transformed MEFs of each genotype (TP53INP1 + / + and TP53INP1 -/-) were irradiated at 10 Gy or not and analyzed by Western blotting 24 h later. Western blot shows autophagic p62 protein and vinculin (Housekeeping gene). *Right*: Quantification of two independent experiments shows the relative quantity of p62 normalized by vinculin.

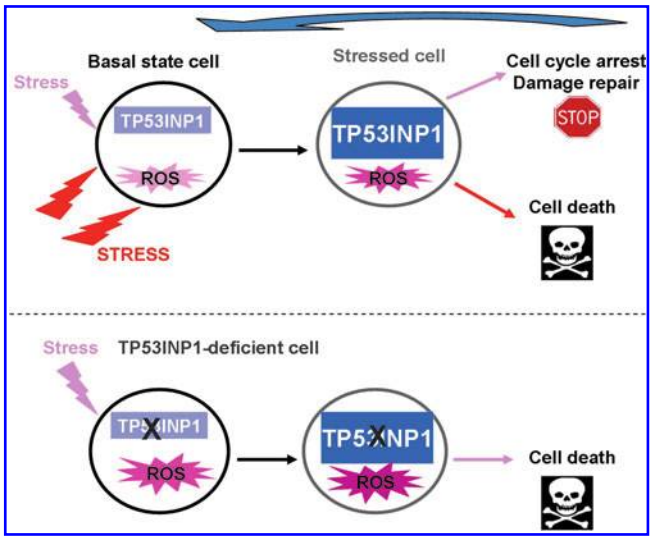

FIG. 10. Proposed model for dual function of TP53INP1 in cell death. *(Top)* Stress response involves high expression of TP53INP1 which participates either in cell cycle arrest permitting damage repair or in cell death depending on stress duration and intensity. *(Bottom)* In the absence of TP53INP1, cell elimination by apoptosis is favored owing to lack of participation of TP53INP1 in stress resolution. (To see this illustration in color the reader is referred to the web version of this article at www.liebertonline.com/ars).

death depends on abnormal redox status in TP53INP1-deficient cells. As such, this observation is consistent with the knowledge that increased level of ROS promotes apoptosis (9, 46). The relationship between ROS and cell death is complex, since on one hand exposure to high levels of ROS induces cell death, and on the other hand ROS are produced during cell death mostly by mitochondria (34). Dysregulation of ROS levels in the absence of TP53INP1 was previously reported by our laboratory (7, 16) and is further documented in the current analysis. We show here that this dysregulation is probably the result of disequilibrium (or perturbations) in small molecule antioxidant concentrations. In particular, vitamin C (ascorbate) is highly lacking in most TP53INP1-deficient cells and tissues. It is known that ascorbate and glutathione levels reflect a steady state balance between their synthesis and loss (17, 27). The liver is the major source of both these antioxidant molecules in the bloodstream and for supply to other tissues. Interestingly, liver and thymus are organs were balance of ascorbate and glutathione levels differs from the other tested organs. Our data suggest a higher *de novo* production of ascorbate in TP53INP1-deficient liver that could be due to a higher need owing to higher ROS level in TP53INP1-deficient mice. Moreover, we observe that ascorbate level is increased in WT liver upon irradiation, suggesting higher *de novo* production based on decreased level of glutathione, as described by Martensson and Meister (27). This increased level of ascorbate is not observed in the TP53INP1-deficient liver upon irradiation; on the contrary, ascorbate level drops whereas glutathione level increases, suggesting a higher systemic use of ascorbate and radiation-induced production of glutathione. Our data also show a higher level of ascorbate in TP53INP1-deficient thymus, contrary to thymocytes. This suggests a higher provision of ascorbate in TP53INP1-deficient thymus, further suggesting a protection of thymus against oxidative stress. Nevertheless, in spite of this protective microenvironment, irradiation stress provides a higher production of ROS in deficient thymocytes compared to WT. Altogether, our data demonstrate a profound dysregulation of antioxidant balances in the absence of TP53INP1. The dysregulation of reduced glutathione is the foremost defect highlighted by this study. We tested culture medium complementation with other antioxidants molecules than NAC, Trolox (a water-soluble vitamin E derivative) and Ebselen (an organo-selenium compound possessing antioxidant properties). Both were able to decrease ROS content in WT but not in TP53INP1-deficient cells, and they were unable to prevent apoptosis (data not shown). Hence, the sensitivity of TP53INP1-deficient cells to cell death is only corrected by NAC which corrects their defect in glutathione. We can therefore propose that loss of glutathione in TP53INP1-/- cells is the critical factor in sensitizing these cells to oxidative stress. Whether this loss is the cause or consequence of constitutive oxidative stress in TP53INP1-deficient animals is currently under investigation.

This study points to the question of basal role of TP53INP1 in thymus (*i.e.*, even in the absence of stress). TP53INP1 is highly expressed in the thymus and other lymphoid organs, contrary to most of tested organs where it is moderately expressed ((8) and unpublished data). Why TP53INP1 is highly expressed in immune cells in the absence of acute stress is a matter of debate. Does it mean that thymus is in permanent stress and that T cells in development are stressed cells? This point of view could be accepted since DNA double-strand breaks are occurring in the course of TCR genes rearrangement, constituting a feature of DNA damage prone to provoke a stress response. In addition, thymocytes are in permanent "stress" of selection, and only those which express a TCR recognizing a self peptide in the context of self MHC are positively selected and survive. Most T cells in development die, which underlies a high rate of apoptosis in the thymus. Strikingly, this study pinpoints an elevated ascorbate content in the thymus, suggesting that a protection against oxidative stress has been selected in this organ, resulting in a well-adapted response to chronic stress underlying T cells maturation events. Hence, we can propose that TP53INP1 contributes to homeostasis in the thymus even in the absence of exogenous acute stress, thereby exerting pro-survival functions. Interestingly, such contribution to cell homeostasis in nonstressed cells is also proposed in the case of p53 (see accompanying reviews in the Forum).

Duality between pro-survival and pro-apoptotic function is also observed in the case of p53, depending on the cell and stress contexts (20). Management of cell survival/death is not the sole function of p53 which displays duality. Indeed, it has been well documented that p53 can play a dual role during oxidative stress (antioxidant or pro-oxidant), depending on the cell outcome (survival versus apoptosis, respectively) (37). In addition, p53 plays a dual function during autophagy, either as a facilitator owing to its transcriptional role in the nucleus or an inhibitor in the cytoplasm (41). Autophagy is reported to be a protective process for cell homeostasis and prevention of various pathologies, including cancer (24). Interestingly, we evidence here a defect in basal autophagy in TP53INP1-deficient cells as well as upon irradiation. These data are consistent with the protective pro-survival role of autophagy (5) which is certainly missing in TP53INP1-deficient

cells, favoring their commitment to death. Therefore, our study provides a new molecular player in autophagy. Deciphering the role of TP53INP1 in regulation of cell redox status in link with modulation of autophagy will help to highlight the complex relationship between ROS and autophagy (38).

In conclusion, the stress response is complex, depending on cellular context, intensity and duration of stress, in part because the function of proteins dedicated to stress resolution could be multiple. We exemplify this point in the present study by demonstrating that TP53INP1, previously reported as a pro-apoptotic protein, is also involved in protection against induced cell death upon death stimuli. Furthermore, we demonstrate here that the increase of ROS load associated with absence of TP53INP1 sensitizes cells to cell death induced by agents known to provoke an oxidative stress. This latter activity is proposed to be used in cancer therapy (35). Therefore, novel strategies in cancer therapy aiming to exploit this feature can be developed in the case of cancers associated with loss of TP53INP1.

Acknowledgments

We thank Gilles Warcollier and Fabrice Gianardi for animal care, Sophie Vasseur and Tak Mak for p53-deficient mice on C57BL/6 background, Rose Patricia Spoto for help in genotyping, and Emilie Ricquebourg for her valuable technical assistance in antioxidants dosage.

The authors are supported by Institut National de la Santé et de la Recherche Médicale, Centre National de la Recherche Scientifique, Institut National du Cancer, Association pour la Recherche sur le Cancer, La Ligue Nationale Contre le Cancer, and Fondation pour la Recherche Médicale.

Author Disclosure Statement

No competing financial interests exist.

References

1. Anderson ME. Determination of glutathione and glutathione disulfide in biological samples. *Methods Enzymol* 113: 548–555, 1985.
2. Ashwell JD, Lu FW, and Vacchio MS. Glucocorticoids in T cell development and function. *Annu Rev Immunol* 18: 309–345, 2000.
3. Barbati S, Clément JL, Fréjaville C, Bouteiller JC, Tordo P, Michel JC, and Yadan JC. 31P-labeled pyrroline N-oxides: Synthesis of 5-diethylphosphone-5-methyl-1-pyrroline N-oxide (DEPMPO) by oxidation of diethyl (2-methylpyrrolidin-2-yl)phosphonate. *Synthesis* 2036–2040, 1999.
4. Bieri JG, Tolliver TJ, and Catignani GL. Simultaneous determination of alpha-tocopherol and retinol in plasma or red cells by high pressure liquid chromatography. *Am J Clin Nutr* 32: 2143–2149, 1979.
5. Boya P, Gonzalez–Polo RA, Casares N, Perfettini JL, Dessen P, Larochette N, Metivier D, Meley D, Souquere S, Yoshimori T, Pierron G, Codogno P, and Kroemer G. Inhibition of macroautophagy triggers apoptosis. *Mol Cell Biol* 25: 1025–1040, 2005.
6. Breen AP and Murphy JA. Reactions of oxyl radicals with DNA. *Free Radic Biol Med* 18: 1033–1077, 1995.
7. Cano CE, Gommeaux J, Pietri S, Culcasi M, Garcia S, Seux M, Barelier S, Vasseur S, Spoto RP, Pebusque MJ, Dusetti NJ, Iovanna JL, and Carrier A. Tumor protein 53-induced nuclear protein 1 is a major mediator of p53 antioxidant function. *Cancer Res* 69: 219–226, 2009.
8. Carrier A, Nguyen C, Victorero G, Granjeaud S, Rocha D, Bernard K, Miazek A, Ferrier P, Malissen M, Naquet P, Malissen B, and Jordan BR. Differential gene expression in CD3epsilon- and RAG1-deficient thymuses: Definition of a set of genes potentially involved in thymocyte maturation. *Immunogenetics* 50: 255–270, 1999.
9. Circu ML and Aw TY. Reactive oxygen species, cellular redox systems, and apoptosis. *Free Radic Biol Med* 48: 749–762, 2010.
10. Clarke AR, Purdie CA, Harrison DJ, Morris RG, Bird CC, Hooper ML, and Wyllie AH. Thymocyte apoptosis induced by p53-dependent and independent pathways. *Nature* 362: 849–852, 1993.
11. Culcasi M, Rockenbauer A, Mercier A, Clément JL, and Pietri S. The line asymmetry of electron spin resonance spectra as a tool to determine the cis:trans ratio for spin-trapping adducts of chiral pyrrolines N-oxides: The mechanism of formation of hydroxyl radical adducts of EMPO, DEPMPO, and DIPPMPO in the ischemic-reperfused rat liver. *Free Radic Biol Med* 40: 1524–1538, 2006.
12. Duling DR. Simulation of multiple isotropic spin-trap EPR spectra. *J Magn Reson B* 104: 105–110, 1994.
13. Dusetti NJ, Tomasini R, Azizi A, Barthet M, Vaccaro MI, Fiedler F, Dagorn JC, and Iovanna JL. Expression profiling in pancreas during the acute phase of pancreatitis using cDNA microarrays. *Biochem Biophys Res Commun* 277: 660–667, 2000.
14. Erlacher M, Michalak EM, Kelly PN, Labi V, Niederegger H, Coultas L, Adams JM, Strasser A, and Villunger A. BH3-only proteins Puma and Bim are rate-limiting for gamma-radiation- and glucocorticoid-induced apoptosis of lymphoid cells *in vivo*. *Blood* 106: 4131–4138, 2005.
15. Gironella M, Seux M, Xie MJ, Cano C, Tomasini R, Gommeaux J, Garcia S, Nowak J, Yeung ML, Jeang KT, Chaix A, Fazli L, Motoo Y, Wang Q, Rocchi P, Russo A, Gleave M, Dagorn JC, Iovanna JL, Carrier A, Pebusque MJ, and Dusetti NJ. Tumor protein 53-induced nuclear protein 1 expression is repressed by miR-155, and its restoration inhibits pancreatic tumor development. *Proc Natl Acad Sci USA* 104: 16170–16175, 2007.
16. Gommeaux J, Cano C, Garcia S, Gironella M, Pietri S, Culcasi M, Pebusque MJ, Malissen B, Dusetti N, Iovanna J, and Carrier A. Colitis and colitis-associated cancer are exacerbated in mice deficient for tumor protein 53-induced nuclear protein 1. *Mol Cell Biol* 27: 2215–2228, 2007.
17. Griffith OW. Biologic and pharmacologic regulation of mammalian glutathione synthesis. *Free Radic Biol Med* 27: 922–935, 1999.
18. Hershko T, Chaussepied M, Oren M, and Ginsberg D. Novel link between E2F and p53: proapoptotic cofactors of p53 are transcriptionally upregulated by E2F. *Cell Death Differ* 12: 377–383, 2005.
19. Hogquist KA, Baldwin TA, and Jameson SC. Central tolerance: Learning self-control in the thymus. *Nat Rev Immunol* 5: 772–782, 2005.
20. Janicke RU, Sohn D, and Schulze–Osthoff K. The dark side of a tumor suppressor: Anti-apoptotic p53. *Cell Death Differ* 15: 959–976, 2008.
21. Jiang PH, Motoo Y, Garcia S, Iovanna JL, Pebusque MJ, and Sawabu N. Down-expression of tumor protein p53-induced nuclear protein 1 in human gastric cancer. *World J Gastroenterol* 12: 691–696, 2006.

22. Jiang PH, Motoo Y, Iovanna JL, Pebusque MJ, Xie MJ, Okada G, and Sawabu N. Tumor protein p53-induced nuclear protein 1 (TP53INP1) in spontaneous chronic pancreatitis in the WBN/Kob rat: Drug effects on its expression in the pancreas. *J. Pancreas* 5: 205–216, 2004.
23. Klein L, Hinterberger M, Wirnsberger G, and Kyewski B. Antigen presentation in the thymus for positive selection and central tolerance induction. *Nat Rev Immunol* 9: 833–844, 2009.
24. Levine B and Kroemer G. Autophagy in the pathogenesis of disease. *Cell* 132: 27–42, 2008.
25. Lowe SW, Schmitt EM, Smith SW, Osborne BA, and Jacks T. p53 is required for radiation-induced apoptosis in mouse thymocytes. *Nature* 362: 847–849, 1993.
26. Maeda S, Kamata H, Luo JL, Leffert H, and Karin M. IKK-beta couples hepatocyte death to cytokine-driven compensatory proliferation that promotes chemical hepatocarcinogenesis. *Cell* 121: 977–990, 2005.
27. Martensson J and Meister A. Glutathione deficiency increases hepatic ascorbic acid synthesis in adult mice. *Proc Natl Acad Sci USA* 89: 11566–11568, 1992.
28. Mathew R, Karp CM, Beaudoin B, Vuong N, Chen G, Chen HY, Bray K, Reddy A, Bhanot G, Gelinas C, Dipaola RS, Karantza–Wadsworth V, and White E. Autophagy suppresses tumorigenesis through elimination of p62. *Cell* 137: 1062–1075, 2009.
29. Mizushima N, Yoshimori T, and Levine B. Methods in mammalian autophagy research. *Cell* 140: 313–326, 2010.
30. Nitta T, Murata S, Ueno T, Tanaka K, and Takahama Y. Thymic microenvironments for T-cell repertoire formation. *Adv Immunol* 99: 59–94, 2008.
31. Okamura S, Arakawa H, Tanaka T, Nakanishi H, Ng CC, Taya Y, Monden M, and Nakamura Y. p53DINP1, a p53-inducible gene, regulates p53-dependent apoptosis. *Mol Cell* 8: 85–94, 2001.
32. Omaye ST, Turnbull JD, and Sauberlich HE. Selected methods for the determination of ascorbic acid in animal cells, tissues, and fluids. *Methods Enzymol* 62: 3–11, 1979.
33. Opferman JT. Apoptosis in the development of the immune system. *Cell Death Differ* 15: 234–242, 2008.
34. Orrenius S, Gogvadze V, and Zhivotovsky B. Mitochondrial oxidative stress: Implications for cell death. *Annu Rev Pharmacol Toxicol* 47: 143–183, 2007.
35. Pelicano H, Carney D, and Huang P. ROS stress in cancer cells and therapeutic implications. *Drug Resist Updat* 7: 97–110, 2004.
36. Pietri S, Liebgott T, Fréjaville C, Tordo P, and Culcasi M. Nitrone spin traps and their pyrrolidine analogs in myocardial reperfusion injury: Hemodynamic and ESR implications—evidence for a cardioprotective phosphonate effect for 5-(diethoxyphosphoryl)-5-methyl-1-pyrroline N-oxide in rat hearts. *Eur J Biochem* 254: 256–265, 1998.
37. Sablina AA, Budanov AV, Ilyinskaya GV, Agapova LS, Kravchenko JE, and Chumakov PM. The antioxidant function of the p53 tumor suppressor. *Nat Med* 11: 1306–1313, 2005.
38. Scherz–Shouval R and Elazar Z. ROS, mitochondria and the regulation of autophagy. *Trends Cell Biol* 17: 422–427, 2007.
39. Strasser A, Harris AW, and Cory S. bcl-2 transgene inhibits T cell death and perturbs thymic self-censorship. *Cell* 67: 889–899, 1991.
40. Takahama Y. Journey through the thymus: Stromal guides for T-cell development and selection. *Nat Rev Immunol* 6: 127–135, 2006.
41. Tasdemir E, Chiara Maiuri M, Morselli E, Criollo A, D'Amelio M, Djavaheri–Mergny M, Cecconi F, Tavernarakis N, and Kroemer G. A dual role of p53 in the control of autophagy. *Autophagy* 4: 810–814, 2008.
42. Tomasini R, Samir AA, Carrier A, Isnardon D, Cecchinelli B, Soddu S, Malissen B, Dagorn JC, Iovanna JL, and Dusetti NJ. TP53INP1s and homeodomain-interacting protein kinase-2 (HIPK2) are partners in regulating p53 activity. *J Biol Chem* 278: 37722–37729, 2003.
43. Tomasini R, Samir AA, Pebusque MJ, Calvo EL, Totaro S, Dagorn JC, Dusetti NJ, and Iovanna JL. P53-dependent expression of the stress-induced protein (SIP). *Eur J Cell Biol* 81: 294–301, 2002.
44. Tomasini R, Samir AA, Vaccaro MI, Pebusque MJ, Dagorn JC, Iovanna JL, and Dusetti NJ. Molecular and functional characterization of the stress-induced protein (SIP) gene and its two transcripts generated by alternative splicing. SIP induced by stress and promotes cell death. *J Biol Chem* 276: 44185–44192, 2001.
45. Tomasini R, Seux M, Nowak J, Bontemps C, Carrier A, Dagorn JC, Pebusque MJ, Iovanna JL, and Dusetti NJ. TP53INP1 is a novel p73 target gene that induces cell cycle arrest and cell death by modulating p73 transcriptional activity. *Oncogene* 24: 8093–8104, 2005.
46. Trachootham D, Lu W, Ogasawara MA, Nilsa RD, and Huang P. Redox regulation of cell survival. *Antioxid Redox Signal* 10: 1343–1374, 2008.
47. Yoshida K, Liu H, and Miki Y. Protein kinase C delta regulates Ser46 phosphorylation of p53 tumor suppressor in the apoptotic response to DNA damage. *J Biol Chem* 281: 5734–5740, 2006.

Address correspondence to:
Dr. Alice Carrier
INSERM U624
Case 915 Parc Scientifique de Luminy
13288 Marseille Cedex 9
France

E-mail: alice.carrier@inserm.fr

Date of first submission to ARS Central, August 5, 2010; date of final revised submission, January 4, 2011; date of acceptance, January 14, 2011.

Abbreviations Used

7-AAD = 7-amino-actinomycin
DCF-DA = 2′,7′-dichlorofluorescein diacetate
DEPMPO = 5-diethoxyphosphoryl-5-methyl-1-pyrroline *N*-oxide
$DiOC_6$ = 3,3′-dihexyloxacarbocyanine iodide
DP = double-positive
ESR = electron spin resonance
Gy = Gray
MEFs = mouse embryonic fibroblasts
NAC = *N*-acetylcysteine
ROS = reactive oxygen species
TP53INP1 = Tumor Protein 53-Induced Nuclear Protein 1

This article has been cited by:

1. Marcel Culcasi, Laila Benameur, Anne Mercier, Céline Lucchesi, Hidayat Rahmouni, Alice Asteian, Gilles Casano, Alain Botta, Hervé Kovacic, Sylvia Pietri. 2012. EPR spin trapping evaluation of ROS production in human fibroblasts exposed to cerium oxide nanoparticles: Evidence for NADPH oxidase and mitochondrial stimulation. *Chemico-Biological Interactions* **199**:3, 161-176. [CrossRef]